International Journal of Trend in Scientific Research and Development (IJTSRD)
Volume 9 Issue 4, Jul-Aug 2025 Available Online: www.ijtsrd.com e-ISSN: 2456 – 6470

Reinforcement Learning-Based Reference Control of D-STATCOM for Reactive Power Compensation and Power Quality Enhancement in Autonomous Microgrids

Arti[1], Pramod Kumar Rathore[2]

[1]M Tech Scholar, RKDF College of Engineering, Bhopal, Madhya Pradesh, India
[2]Assistant Professor, RKDF College of Engineering, Bhopal, Madhya Pradesh, India

ABSTRACT

This paper presents a unique online reference control technique for distribution static compensators that use the reinforcement learning algorithm. The goal of this strategy is to address the power quality issues that develop in microgrids. The unique controller is designed to correct reactive power, harmonics, and unbalanced load current in a microgrid by using voltage and current characteristics. The current-based controller use the quadrature axis (q-axis) and the zero axis (0-axis) to correct for unequal load current in scattered resource networks. In contrast, the voltage controller is used to change the desired value of the reactive power reference. The control technique was developed and implemented in an autonomous microgrid with a weak AC-supply (non-stiff source) distribution system. It has been tested with various load circumstances and three-phase fault scenarios. Several situations are analyzed, and simulation results for a variety of settings are discussed. The report also contains a full evaluation of the effectiveness of the developed online secondary control mechanism.

KEYWORDS: *DSTATCOM control, microgrid management, online control, power quality enhancement, reactive power control, reinforcement learning.*

How to cite this paper: Arti | Pramod Kumar Rathore "Reinforcement Learning-Based Reference Control of D-STATCOM for Reactive Power Compensation and Power Quality Enhancement in Autonomous Microgrids" Published in International Journal of Trend in Scientific Research and Development (ijtsrd), ISSN: 2456-6470, Volume-9 | Issue-4, August 2025, pp.685-699, URL: www.ijtsrd.com/papers/ijtsrd97324.pdf

IJTSRD97324

I. INTRODUCTION

Decentralization of power generating systems necessitates widespread installation of dispersed energy resources in electric power grids. These resources enable flexibility and reduce reliance on the traditional monodirectional power grid. The penetration rate of distributed resource (DR) units is rapidly increasing in today's power system network [1], however it is becoming more obvious that the problems of DR use outweigh the benefits. DR has the potential to cause technical challenges, but it also offers several important advantages [2]. The full advantages of DR units are gained when they are operated in both grid-connected and islanded (autonomous) modes. As a result, microgrids may be used to operate DRs as a solution for both individual and autonomous scenarios [3].

Microgrids, on the other hand, have considerable PQ difficulties in autonomous mode because to the variety of linear and nonlinear loads [4]. Some examples include voltage loss, harmonics, voltage sag, and voltage swell. To address and overcome these difficulties, numerous standards have been established and implemented for operators and utilities [5]. The reduction of unwanted PQ issues may be achieved by careful monitoring and then using appropriate power electronic devices for compensation. However, this is just one of many viable options [6]. When compared to a conventional outline network, the Microgird has its own power quality issues due to network setup, special operating characteristics, storage kinds, and discovery elements. PQ problems are typically classified into three types: microsources (i.e., oscillations in the output of renewable energy sources), harmonics provided by power electronics used in microgrids, and voltage sags caused by increasing load reactive power demands. DSTATCOM is one of the devices

that may help overcome PQ concerns in microgrids [7].

Various control strategies for the functioning of DRs, including voltage control and unbalanced currents, have been presented and addressed. The primary strategies that have been extensively published in the literature include reactive power theory [8], synchronous reference frame theory [9], modified p-q theory [10], d-q axis theory [11], [12], and reference current estimation techniques by preserving the voltage of dc links. These approaches are based on sophisticated computations and often include a series of low-pass filters, which causes a delay in the computation of reference currents and hence a delayed dynamic response of DSTATCOM.

Controlling DSTATCOM using a least mean square-based adaptive linear element is proposed in [7]. This method's major contribution is to compensate for reactive power, harmonics, and imbalanced load current in an isolated system using a diesel generator. To achieve voltage regulation at the dc-bus of a Voltage-Sourced Converter (VSC), a positive sequence of load current in the fundamental frequency was delivered using a PI controller. VSC is also controlled using a hysteresis-based Pulse Width Modulation (PWM) control approach, which involves regulating source currents to match reference currents. Furthermore, Kannan et al. [13] proposed a topology for DSTATCOM applications with non-stiff sources. This architecture allows DSTATCOM to have a lower dc-link voltage while maintaining its correction capacity. Additionally, the average switching frequency of the DSTATCOM switches is reduced. Asynchronous reference frame theory for three-phase four-wire DSTATCOM incorporates VSC and a dc link capacitor, as detailed in [14]. DSTATCOM employs this method for source harmonic reduction, reactive power, and neutral current compensation at the PCC.

In [15], a Neural Network (NN) operated DSTATCOM with a dSPACE processor for voltage management or power factor correction is described. Other aims of the NN controlled approach were load balancing, harmonic current removal, and neutral current compensation. Later, [16] described a coordinated control technique in a microgrid that included communication in the DR and DSTATCOM loops. This approach relies on voltage sag and power flow in the line. Power flow and voltage at various feeder sites are sent to the DSTATCOM, which modulates reactive power compensation. To apply this strategy, the communication channel must be available.

This work describes a unique online technique for adjusting (reference) tracking of DSTATCOM set points in microgrids by monitoring PCC voltage and DRs currents. The Reinforcement Learning (RL) algorithm provides online control of DSTATCOM, including reactive power, harmonics, and unbalanced load adjustment. The suggested control approach consists of two major components: voltage-based and current-based control schemes. The voltage-base approach modifies DSTATCOM's reactive power reference, while the current-base strategy injects signals via both the quadrature (q-axis) and zero axis (0-axis) of VSC current controllers under imbalanced situations. The main control uses DSTATCOM's local voltage and current to manage the system's voltage and frequency. To compensate for PQ difficulties in the microgrid, the secondary reference control is based on PCC voltage and DRs current signals. The suggested method's main characteristic is that the secondary controller is independent of the primary. This novel technique is ideal for microgrids with a constantly changing topology, which deteriorates the performance of the planned controller.

To sum up, the main contribution of this study are, (1) introducing a novel online control strategy based on RL algorithm, and (2) controlling the PCC voltage besides controlling of DRs' current in order to overcome PQ problems. The proposed strategy does not require to access system model, and also it can be simply adopted to different types of distributed resources such as wind turbine, synchronous generator and voltage source converter in microgrid.

To evaluate the strategy, this control algorithm is applied on a test microgrid system under load switching; single and double-phase unbalanced loads, nonlinear loads as well as three-phase fault conditions. The studied microgrid system includes wind turbine, voltage source converter based DR with dq-current controller, synchronous generator with a governor, and excitation primary control system. The model is simulated, and the findings are thoroughly analyzed. Simulation results reveal that the proposed algorithm is able to compensate the voltage drop and mitigate the unbalanced currents of distributed resources.

As the power demand has been increasing rapidly, power generation and transmission are being affected due to limited resources, environmental restrictions and other losses. The quality of available supply power has a direct economic impact on industrial and domestic sectors which affects the growth of any nation [1]. This issue is more serious

in electronic based systems. The level of harmonics and reactive power demand are popular parameters that specify the degree of distortion and reactive power demand at a particular bus of the utility [2].

II. PROPOSED CONTROL STRATEGY:

The conventional power system makes considerable use of the concepts of main and secondary control [17]. The primary control is done locally and responds promptly. It's designed as a linear controller, especially using a Proportional Integrative (PI) scheme. The secondary control is a higher level of control that defines specified goal values for the primary controllers inside its zone. The set points are established to enhance operational efficiency by maximizing certain criteria such as maintaining a constant voltage level, producing reactive power, or reducing real power loss. This study focuses on the creation of a secondary controller for DSTATCOM that employs the RL algorithm. The control technique provided comprises of two distinct and independent components. The first strategy is voltage control, which attempts to minimize the voltage profile of the PCC voltage. The second technique is current control, which aims to improve the power quality of dispersed resources. Figure 1 shows a block schematic of the control system.

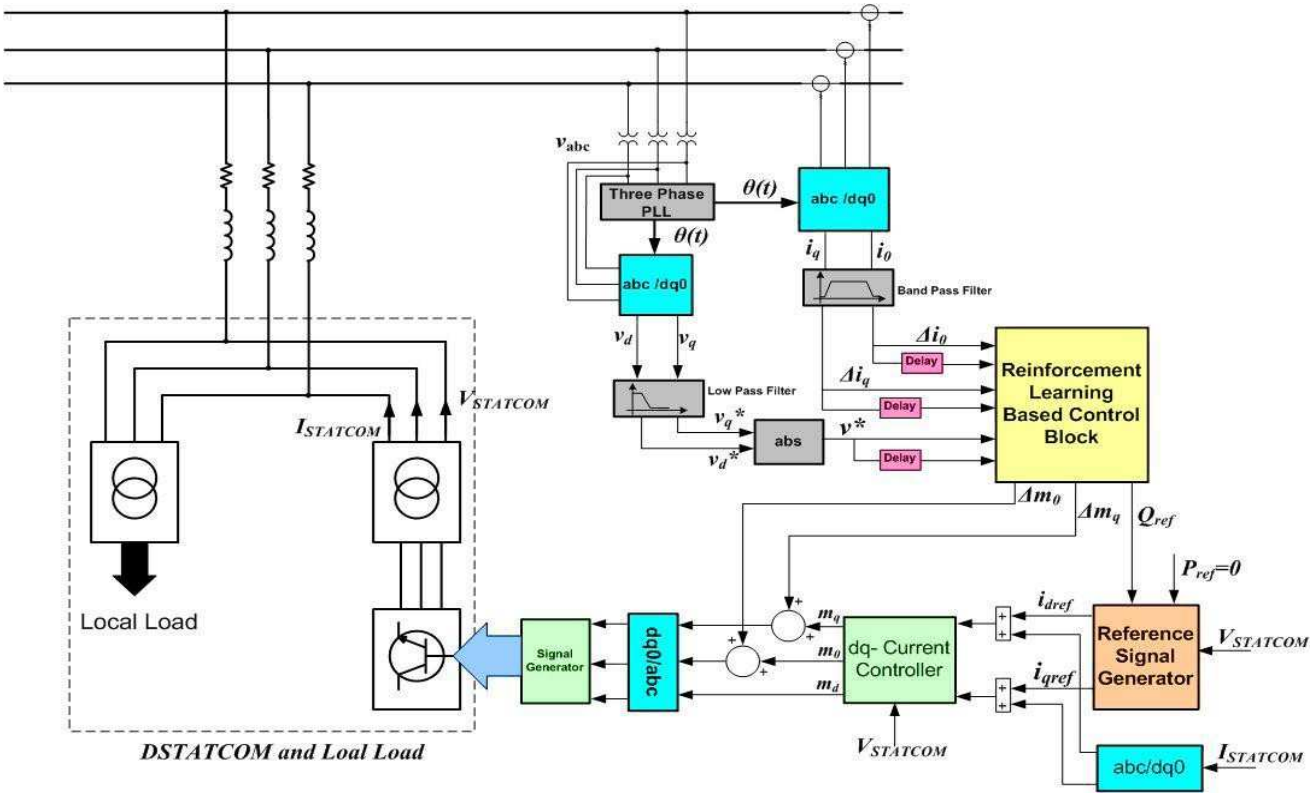

FIGURE 1. Proposed approach for controlling DSTATCOM in microgrid.

A. VOLTAGE-BASE CONTROL STRATEGY

The voltage-base control purpose is to modify the set-point of a STATCOM reactive power reference online in order to acquire a nominal voltage for the PCC bus. Figure 1 depicts the structure of the proposed controller in islanded mode of operation. PCC voltage (V_PCC) is measured and stored in a dq-frame. A three-phase Power Common Coupling (PLL) is utilized to supply the reference angle for the abc/dq block, so the q component of the PCC voltage is zero. In this situation, the d component of the PCC voltages, v_d, should be controlled to achieve the required peak voltage (v_dref). After that, it is compared to the reference signal, and the sum of the error signal square is sent into the designated RL-base controller for regulation. The RL controller output is a reference value for DSTATCOM reactive power production (Q_ref), which is applied to the VSC's reference signal generator, as shown in Fig.1. The set point modification is then performed for each time horizon, T_Cont. This horizon determines the behavior of the RL algorithm, which is chosen based on the best choice and rate of fluctuation of the controllable variables.

B. CURRENT-BASE CONTROL STRATEGY

The current-base control objective is based on online injecting corrective signals ($[\Delta m_d, \Delta m_q]$) into the system through both quadrature axis ($q-axis$) and zero axis ($0-axis$) current controllers of the interface converter; see Fig. 1. This corrective signal injection through the q-axis controller modifies frequency deviation under islanded conditions at the PCC. The injected signal through the zero axis of controller causes unbalancing in

load current, which is provided by DSTATCOM. By this composition, unbalanced current of the generation unit is set to zero. As demonstrated in Fig. 1, DRs' currents (I_{DRS}) are measured and then active, reactive and zero components are derived. Implementing a band pass filter; the DC values of these $dq0$ components are eliminated and the $[\Delta i_d \Delta i_q]$ signals are applied to the proposed control strategy. The output signals of RL controller would be $[\Delta m_d, \Delta m_q]$, which are applied to the gating signal generator of the VSC.

III. REINFORCED LEARNING BASED CONTROLLER

A. REINFORCEMENT LEARNING ALGORITHM

Reinforcement learning [18] is considered as one of the most crucial and effective online control strategies. At the beginning, selection is based on the trial-and-error model. However, after pass time horizon, the algorithm is trained to apply suitable control action on different plants indirectly. For each state in this method, a different control action is applied. For instance, if x_t and u_t denote the system state and system control at time t, the state at time $t + 1$ is given by [19]:

$$x_t + 1 = f(x_t, u_t), u_t \in U, \forall t > 0 \quad (1)$$

For each control action in any intervals, a reward or a punishment is presumed. In other word, if this action improves the system error; a reward will be anticipated for this action; otherwise a punishment will be applied. The selection of reward or punishment is specified by comparison between error in t and $t + 1$. Thus, reward selection at time t for each action is given by:

$$R(x_0, u\{t\}) = \sum_{t=0}^{\infty} \gamma^t r\ (x_t, u_t), \quad (2)$$

where, γ is a value between 0 and $1, 0 < \gamma < 1$, and $r(x, u) \leq B. B$ is the maximum value of the reward and is selected through trial and error.

Using obtained values; a value function is defined. From this function, suitable control signal for the next step will be selected as:

$$V(x) = max_{u(t)}\, R\big(x, u(t)\big) \quad (3)$$

Utilizing Bellman equation [19], the value function is given by:

$$V(x) = max_{u \in U} \left[r(x, u) + \gamma V\left(f(x, u)\right)\right] \quad (4)$$

The optimal control policy is expressed as:

$$[u^*(x) = \arg max_{u \in U} \left[r(x, u) + \gamma V\big(f(x, u)\big)\right] \quad (5)$$

According to the mentioned relation for each interval, a reward or punishment function called Q function can be obtained by:

$$Q(x, u) = r(x, u) + \gamma\, V(f\ (x, u)) \quad (6)$$

Re-express $V(x)$ in terms of this function is given by:

$$V(x) = max_{u \in U}\ Q(x, u), \quad (7)$$

and finally, optimal control policy is obtained by:

$$u^*(x) = \arg max_{u \in U}\ Q(x, u) \quad (8)$$

In the proposed secondary controller, for each pair of input/output signal, three different actions can be taken into account. In each state, adaptation unit must select one single action among all three possible actions. Some of the actions are eliminated through the evaluation of their punishment functions; and therefore, a selection process is applied to the other remained actions.

B. RL METHODOLOGY

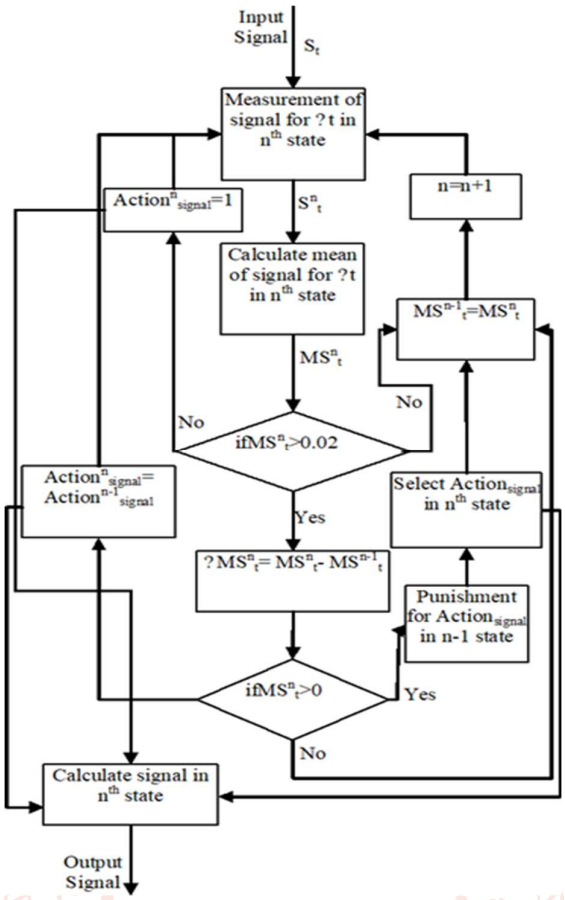

FIGURE 2. Flowchart of the reinforcement learning block algorithm with three input/output pairs.

The flowchart for the secondary reinforcement learning control block is provided in Fig. 2. Using this flowchart, each pair of $(\Delta i_{0,}\Delta m_0)$; $(\Delta i_{q,}\Delta m_q)$; and, $(\Delta v, Q_{ref})$ signals' relation are obtained. Any changes of the input signals cause a change in the outputs. For instance, the voltage deviation Δv over 4ms is measured and the mean absolute error of the PCC voltage is calculated using (9).

$$MS_t^n = \frac{\sum_{m=1}^{N_s} \Delta V_m}{N_s}, (9)$$

where, $(\Delta V_m = [\Delta v_{1,}\Delta v_{2,} \ldots, \Delta v_{Ns}]_m$; Ns; and, MS_t^n are number of samples and the mean absolute error at the state n, respectively. If $MS_t^n < 0.02$, value of the output doesn't change in the next state, whereas for $MS_t^n \geq 0.02$, deviation of $MS(\Delta MS_t^n)$ is given as;

$$\Delta MS_t^n = MS_t^n - MS_t^{n-1} \ (10)$$

where,
MS_t^n and MS_t^{n-1} t are the mean absolute error at state n and $n-1$, respectively.

For $\Delta MS_t^n > 0$, it is obvious that action of the pervious state impairs the voltage error. In this case, punishment is considered for the pervious state action and new action is selected for $n+1$ state. However, if $\Delta MS_t^n \leq 0$, it shows that the pervious state action improves the voltage error. Thus, reward is given for this action and it is selected as the next state action. For each of three input/output signals $[(\Delta i_{0,}\Delta m_0)$; $(\Delta i_{q,}\Delta m_q)$; and, $(\Delta v, Q_{ref})]$ the same procedure is applied independently as described in Fig. 2. Limits of the output signals are considered to prevent of set points increasing from nominal value.

IV. SYSTEM DESCRIPTION

A. SYSTEM TOPOLOGY

Single line diagram of the microgrid system to investigate the proposed algorithm operational behavior is shown in Fig. 3. It consists of radial distribution system which is connected to the utility grid through a 13.8kV line. The distribution system consists of five feeders, three DR units, a DSTATCOM unit feeder, and set of linear and non-linear loads.

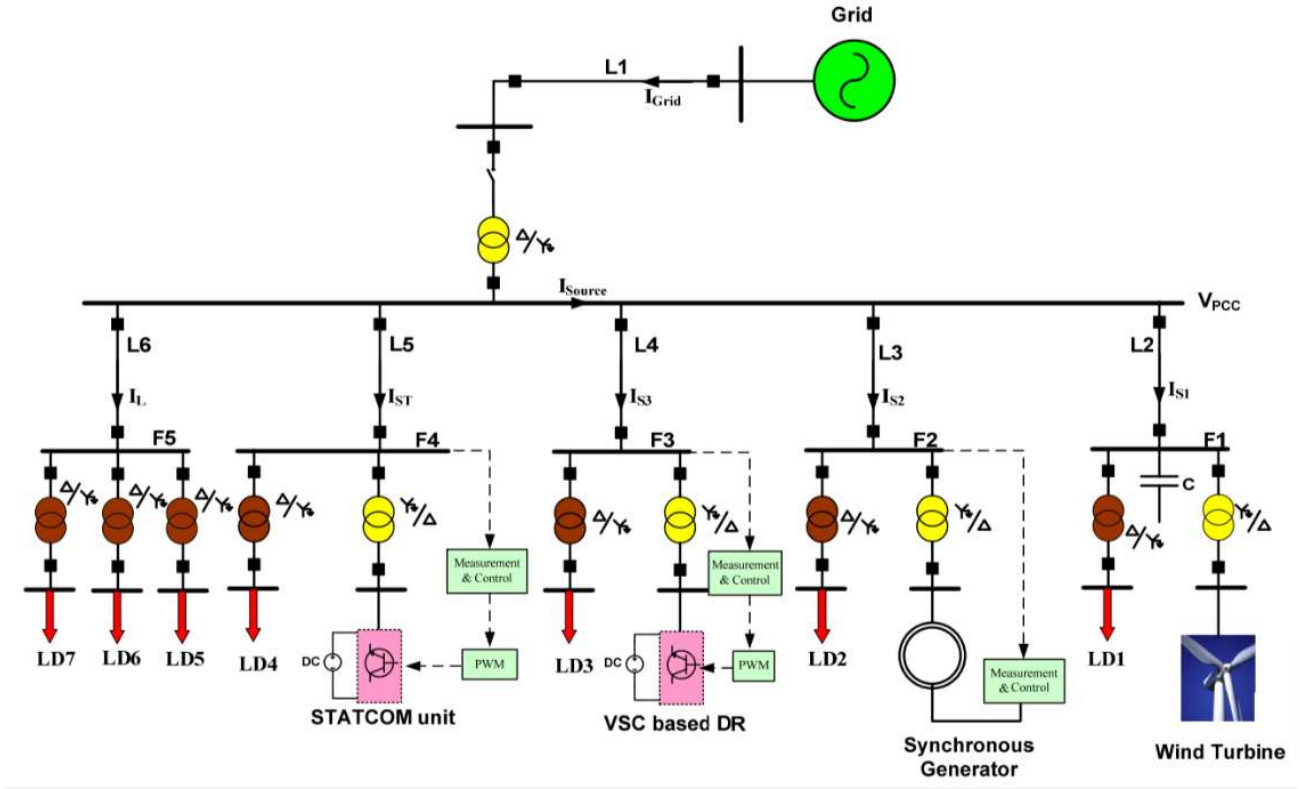

FIGURE 3. Single line diagram of simulated microgrid system.

The 500 kVA substation transformer is configured in delta at the high voltage side and grounded Wye at the low voltage side. The system includes three DR units, i.e. DR_1 (150 kVA), DR_2 (100 kVA) and DR_3 (80 kVA) on the feeders F_1, F_2 and F_3, respectively. DR_1 is a wind turbine with a self-excited asynchronous generator.

DR_2 is a synchronous generator with excitation and governor control system, and DR_3 is a voltage source converter-based distributed generation system controlled by active/reactive control strategy system. A DSTATCOM unit (50 kVA) is connected to F_4 in order to improve the PCC voltage and power quality problem.

The linear loads of LD_1 to LD_4 are supplied through the radial feeders of F_1 to F_4. Loads LD_1 to LD_4 are composed of linear RL branches. LD_5 to LD_7 are supplied through feeder 5, where, LD_5 to LD_6 are linear RL branches and LD_7 is a three-phase full controlled rectifier load. F_1 consists of three-phase capacitor bank which is used as excitation system of the asynchronous generator. The electrical parameters of system, including impedance of lines, transformer parameters and configuration, and rated loads of feeders are given in Fig. 3 and Table 1, respectively.

B. ACTIVE/REACTIVE POWER MANAGEMENT

After islanding from the main grid, frequency of the microgrid is defined by operation points of distributed resources. To restore the system frequency, the synchronous generator is equipped with governor and excitation systems.

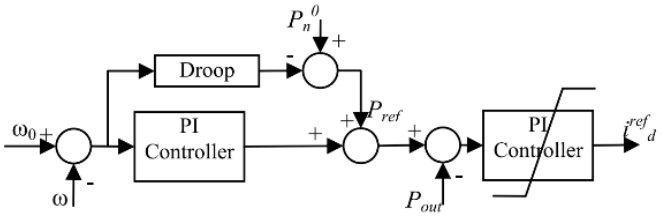

FIGURE 4. Controller of VSC-based distributed generation for active power compensation.

Also, the active power generation of the VSC-based DR unit is specified based on a frequency-drop characteristic and a frequency restoration algorithm. Figure 4 shows a generic active power management block for VSC-based on DR unit in microgrid. The local frequency which is estimated by a PLL is the input parameter of the controller block. The controller output is then output of the block is the reference current for

the d-axis inner current controller of VSC-DR unit, corresponding to the active power reference of the unit. In order to control the reactive power of VSC-based DR unit, voltage-base control strategy is applied; see Fig. 5. Reactive power of the DR unit is controlled to regulate the voltage of DRs' buses at a pre-specified level (normally 1 pu).

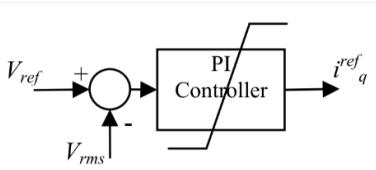

FIGURE 5. Controller of VSC-based distributed generation for reactive power compensation.

V. SIMULATION STUDY AND RESULTS DISCUSSION

To examine and evaluate the proposed control strategy performance, different case studies were exercised. All these studies were conducted for autonomous operation.

Moreover, in grid-connected condition, the proposed method has the same performance of the autonomous mode. In islanding operation, the microgrid is a weak ac-supply distribution system and the frequency control is one of the main issues. To examine both strategies in autonomous mode, three-phase load variation, unbalanced load including single phase and double-phase changes, three-phase fault event, and nonlinear load switching are emulated.

A. SCENARIO 1: LOAD CHANGES IN AUTONOMOUS MODE

The proposed strategy was examined through feeder 5 load changes. In steady state condition, the load of F_1 is 0.75, LD_2 is $0.4 + j0.25$, LD_3 is $0.4 + j0.16$, LD_4 is 0.2 and the load of F_5 is scheduled for $0.4 + j0.12$, all in per unit. From entire demand, $2.15 + j0.53$ system load, 0.75, 0.6 and 0.8pu are supplied by the wind turbine, VSC-based DR and synchronous DR. The system reactive power requirement is distributed among DR units, DSTATCOM and capacitor bank. A $0.2 + j0.1$ pu load in F_5 is increased at $t = 0.4s$ and at $t = 0.8s$. This load is disconnected from F_5. Immediately after load disconnected, production of VSC-based and synchronous DR changes. Fig.6 depicts response of the system to this scenario.

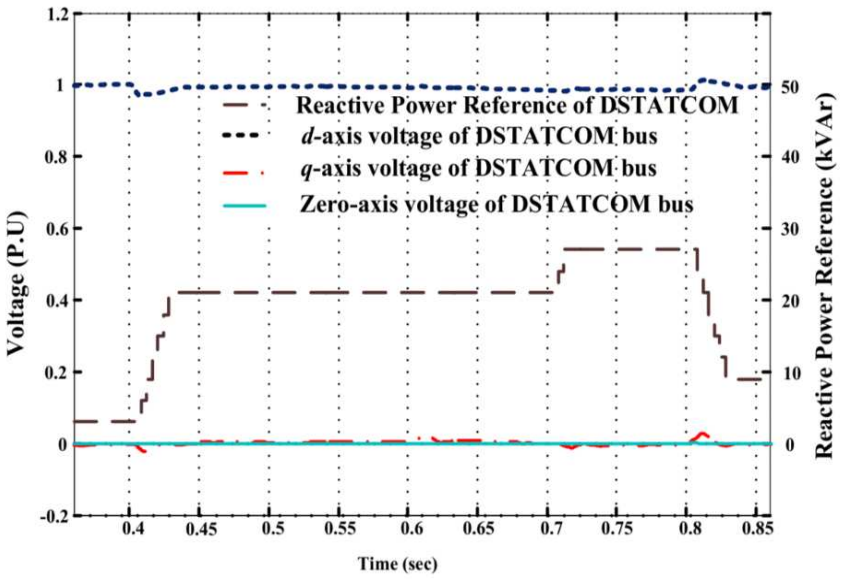

FIGURE 6. System response to scenario 1, (a) Power production of DRs, (b) Reference power of DSTATCOM and dq0 voltage of PCC.

Figures 6(a) and (b) show the active power production of DR units and reactive power reference variation of DSTATCOM with *dq0* PCC voltage, respectively. It is obvious from Fig. 6(b) that the voltage-base RL control strategy will change the reference value of DSTATCOM reactive power.

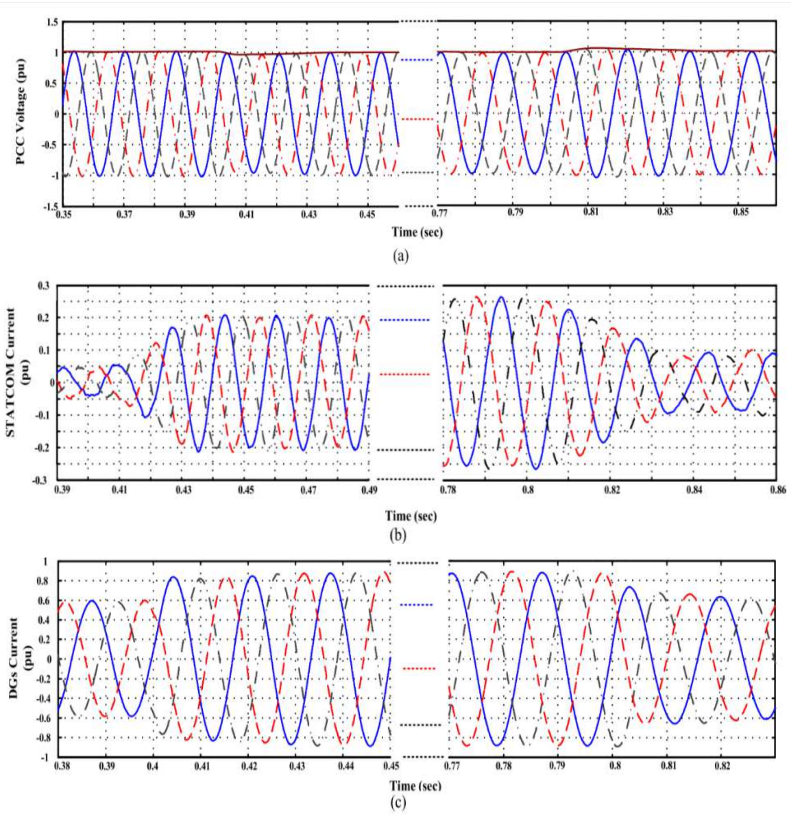

FIGURE 7. System response for scenario 1, (a) PCC voltage, (b) STATCOM current, (c) DGs current (I_{DGs}).

Figures 7(a), (b) and (c) illustrate the voltage of the PCC, DSTATCOM and DRs current before and after load variation, respectively. It is clear that the proposed strategy has controlled voltage of the PCC after load variation by increasing the reactive power generation of DSTATCOM.

B. SCENARIO 2: UNBALANCED LOAD CONDITION

Unbalanced load condition in autonomous mode operation is quite undesirable for distributed generation units. To examine the performance of the proposed algorithm, two unbalanced conditions are presented in this scenario. It is assumed that before switching, the microgrid was operating in steady state condition (*scenario 1*) and the load of F_5 is divided into two equal $0.2 + j0{:}06$ pu loads.

To emulate the unbalanced conditions, supplied load on phase a in one of the F_5 feeders is disconnected at $t = 0.2s$ and then reconnected at $t = 0.3s$.

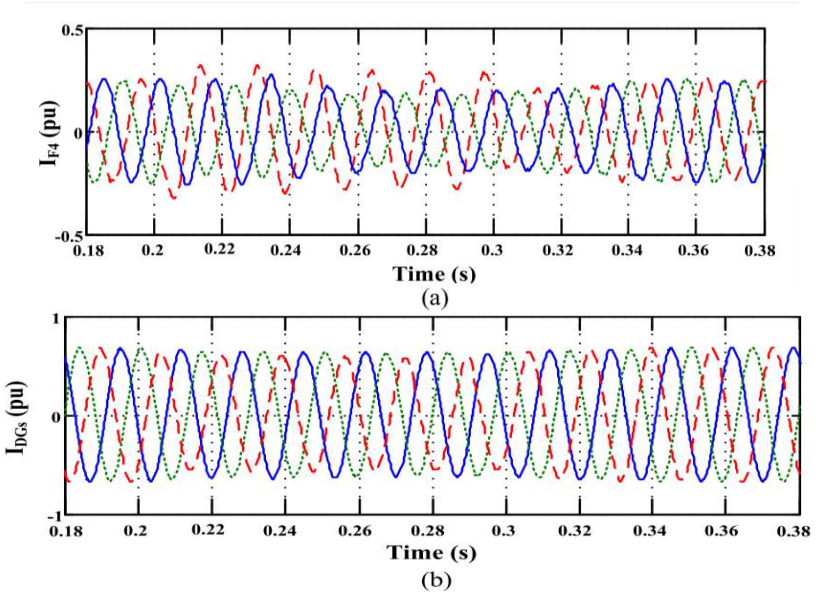

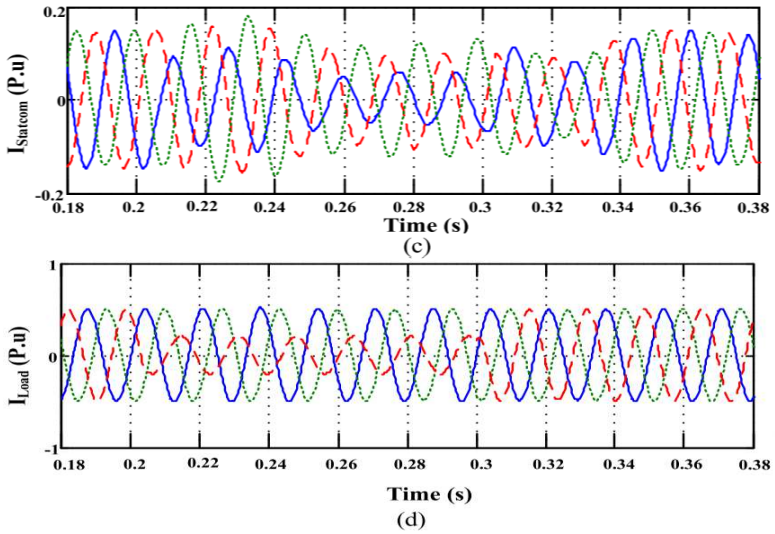

FIGURE 8. System response for scenario 2, (a) Feeder 4 current, (b) DR current, (c) STATCOM current, (d) Load current.

Figures 8 and 9 show the disconnection and connection of load in feeder $F5$ in a period of $0.1s$. Other feeders (feeder 4) DRs, DSTATCOM and loads current are depicted in Figures 8(a) through 8(d), respectively. It can be easily observed that even if the load currents (I_{Load}) become unbalanced, the source currents still remain in balanced condition when the proposed control strategy is applied.

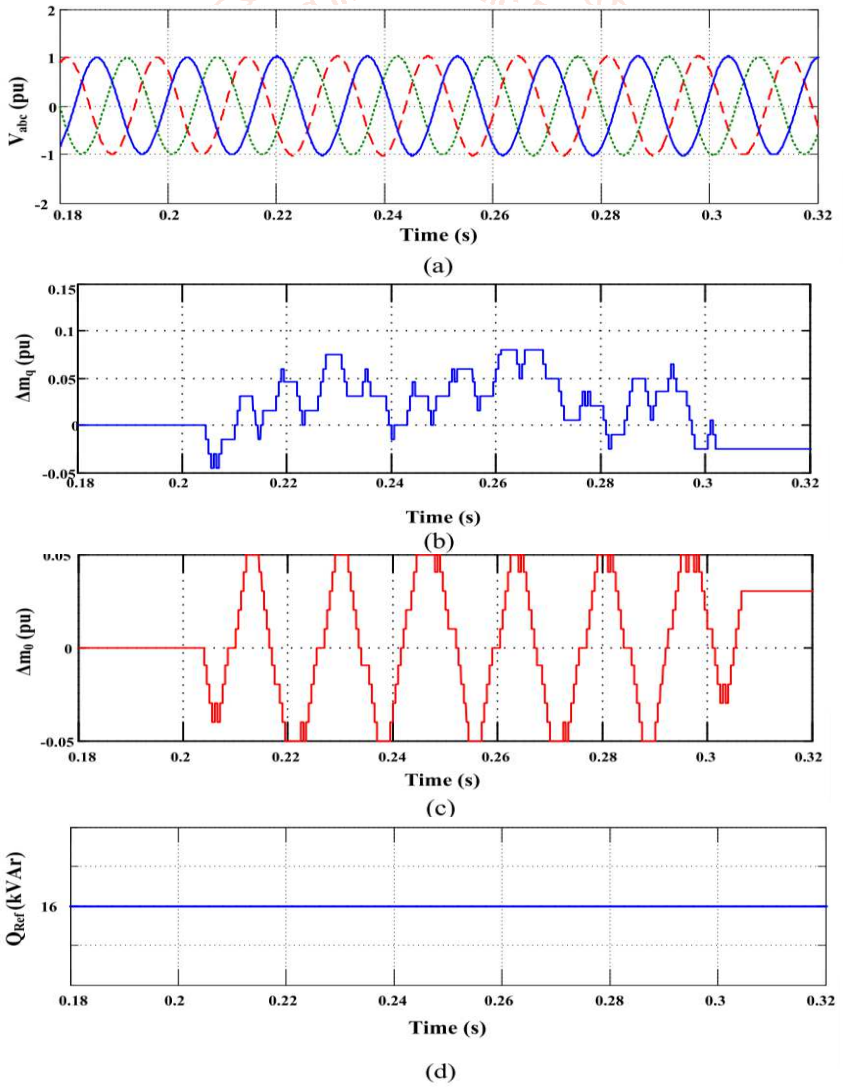

FIGURE 9. System response to scenario 2, (a) The PCC voltage, (b) q axis injected current, (c) zero axis injected current, (d) DSTATCOM reactive power reference.

Figure 9(a) shows the PCC voltage. Δm_q and Δm_0 are illustrated in Figures 9(b) and 9(c), respectively, whereas unbalanced currents of DRs are compensated using these signal variations. Figure 9(d) shows the reference value for DSTATCOM.

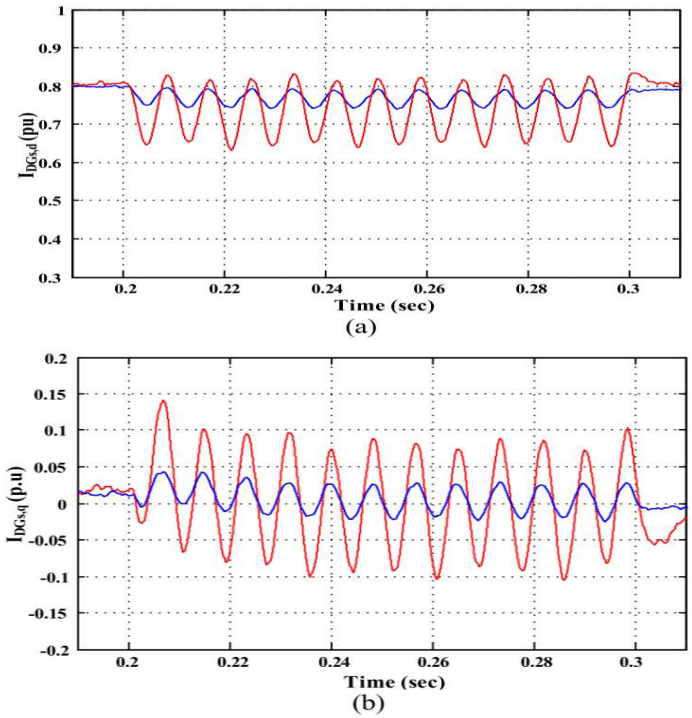

FIGURE 10. System response to scenario 2, (a) d axis current of DRs, (b) q axis current of DRs.

The d and q axes' current of DRs without Δm_q and Δm_0 are shown in Fig. 10. Figure 10 clearly shows that the amplitude variation and signal deviation of d and q-axes' currents are reduced significantly using the proposed control strategy.

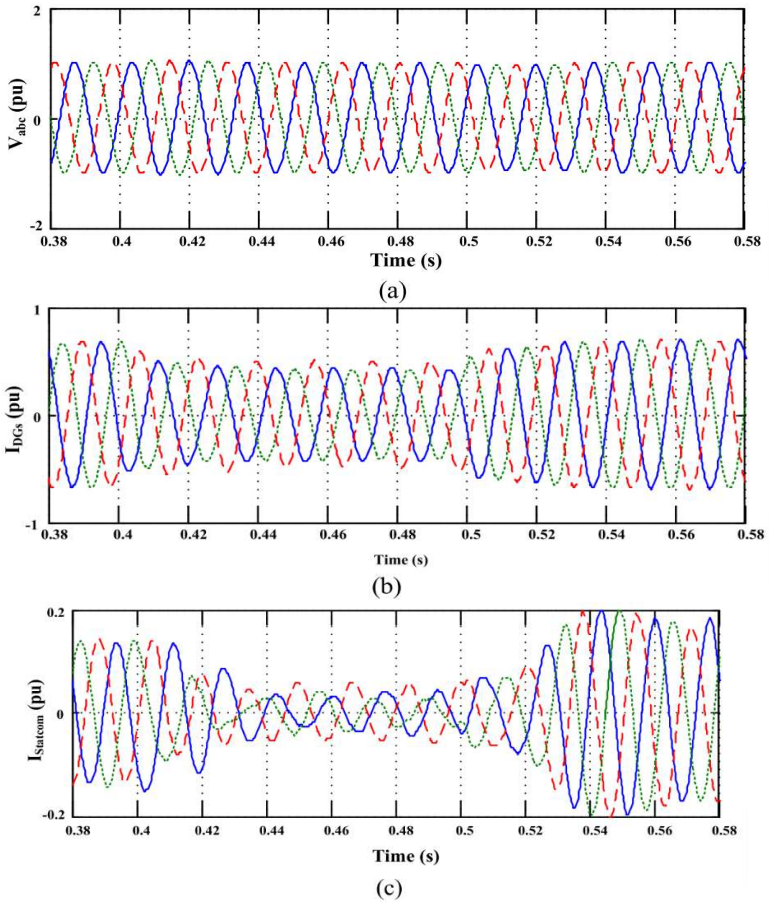

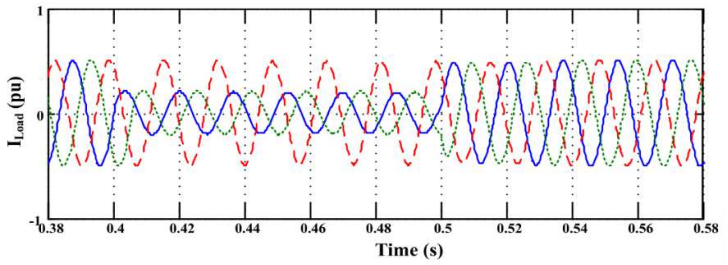

(d)

FIGURE 11. System response to scenario 2, (a) Feeder 4 current, (b) DRs current, (c) STATCOM current, (d) Load current.

For further analysis, another scenario was emulated. At $t = 0.4s$, load is disconnected from phases a and b in one of the F_5 loads and reconnected at $t = 0.5s$. For the time period of $t = 0.4s$ to $t = 0.5s$, dynamic behavior of the Feeder 4, DRs, DSTATCOM and loads currents are presented in Figures 11(a) through 11(d), respectively. It could be readily concluded that DSTATCOM system is able to balance distributed resources currents using the proposed control strategy under this new imposed condition.

C. SCENARIO 3: NON-LINEAR LOAD SWITCHING

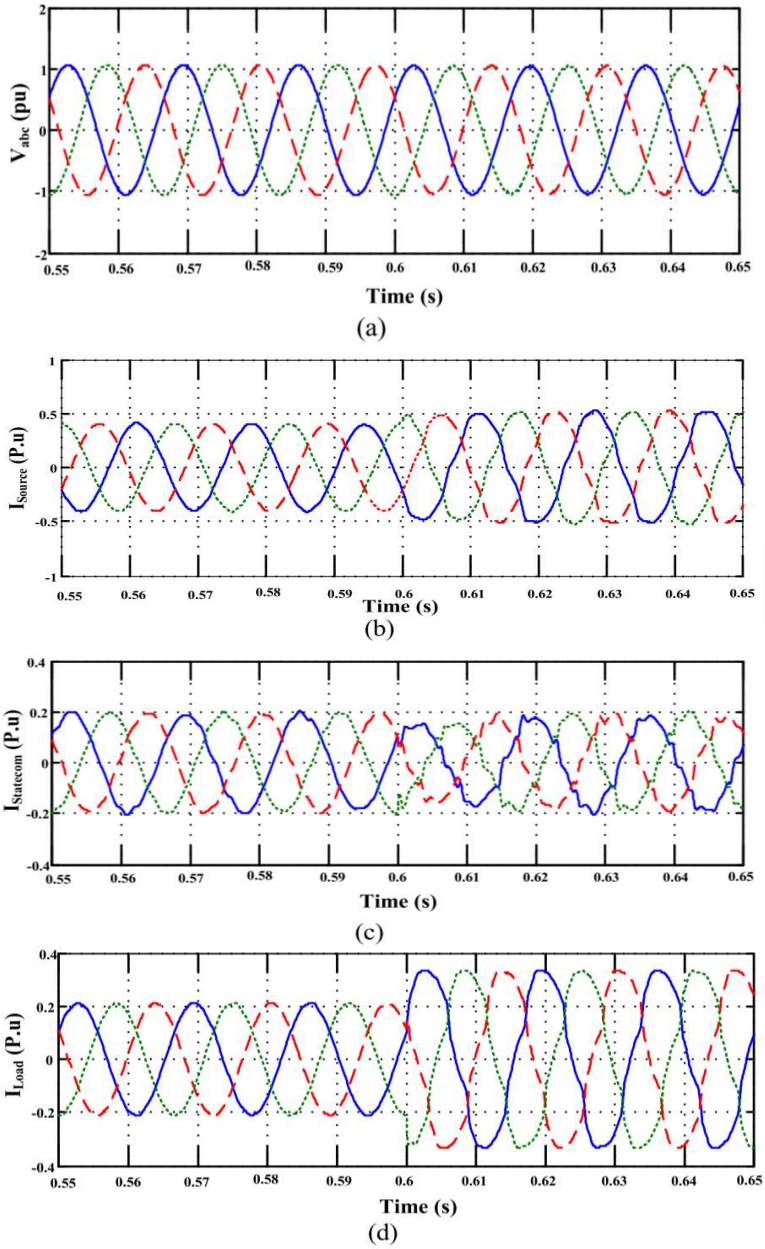

FIGURE 12. System response to scenario 3, (a) Feeder 4 current, (b) DRs current, (c) STATCOM current, (d) Load current.

Non-linear load switching condition is simulated and the results are illustrated in Fig. 12. Figure 12 shows performance of the microgrid with DSTATCOM under nonlinear loading conditions. Before switching, system loading condition was the same as *Scenario 1*. At $t = 0.6s$, a15kW (0.15pu) load was connected to F_5. Simulation results in Fig. 12 reveal that using the proposed algorithm, load harmonic distortions mitigation provided by DSTATCOM and the proposed strategy is able to balance distributed resources currents in nonlinear load switching condition.

D. SCENARIO 4: THREE-PHASE FAULT CONDITION

As the last part of study, three-phase fault condition is simulated. The system behavior due to a fault at $t = 0.3s$ in autonomous operation of the microgrid is shown in Fig.13. Pre-faulting, demand is similar to what discussed in *Scenario 1*. Figure 13(a) shows the PCC voltage before and after fault. It can be observed that the PCC voltage is dropped initially. Figure 13(b) shows the STATCOM current, the current of I_{DRs}. Fault currents (load current) are shown in Figures 13(c) and 13(d), respectively.

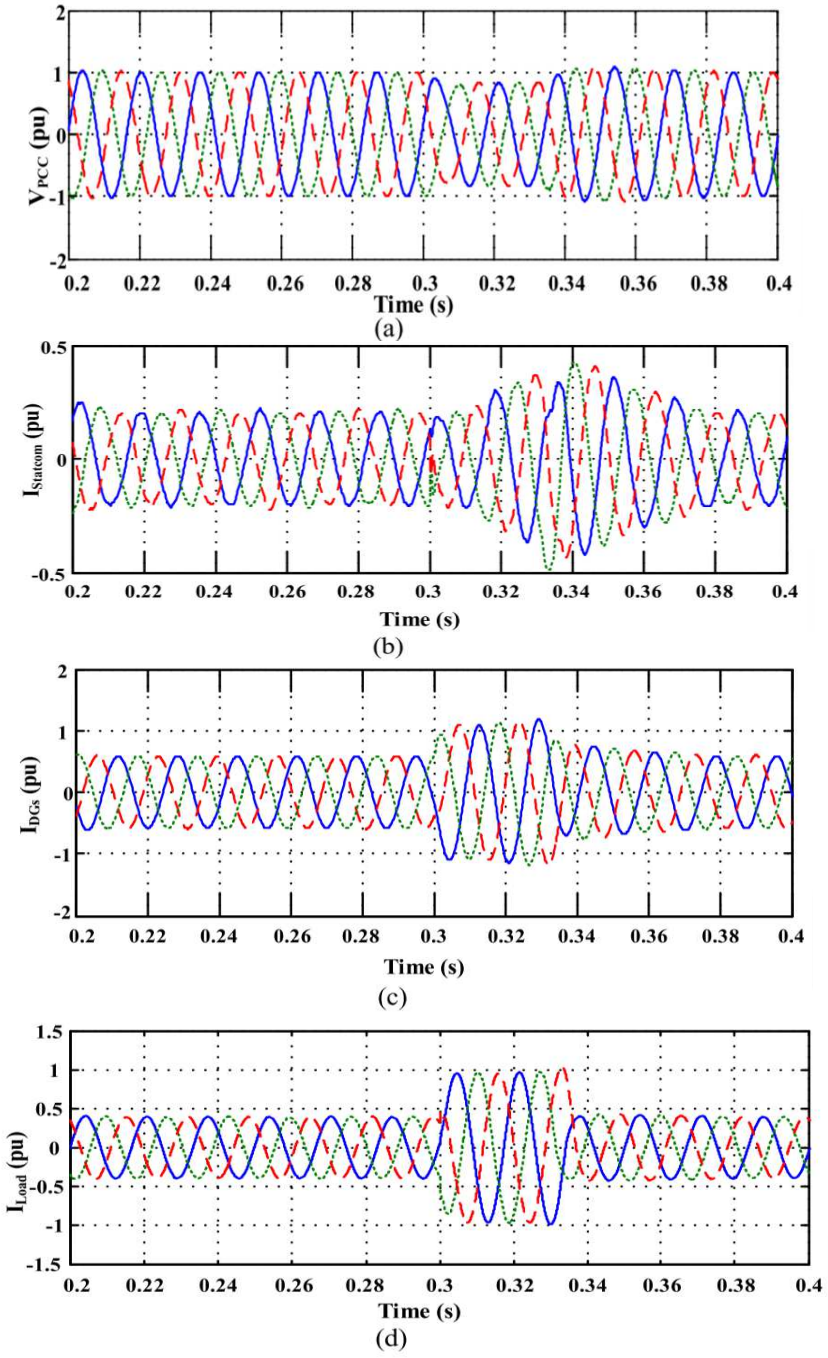

FIGURE 13. System response for scenario 2, (a) Feeder 4 current, (b) DGs current, (c) STATCOM current, (d) Load current.

This section examined the dynamic behavior of a multi DR microgrid system with DSTATCOM, under linear and nonlinear load switching, unbalanced load and three phase fault conditions. The voltage-base control strategy adjusts the reactive power output of DSTATCOM based on the PCC voltage of the microgrid. However, the current-base strategy is used to compensate the unbalanced currents of DRs. The simulation results of tested microgrid under all of the conditions validated the performance and robustness of the proposed control strategy.

VI. CONCLUSION

This study created and investigated a novel online approach for reactive power management of DSTATCOM using the secondary control concept and the reinforcement learning algorithm in a microgrid. The main goal was to compensate for reactive power, harmonics, and uneven load currents. The recommended online reference control approach was based on voltage and current profile modifications. The voltage controller monitors the PCC voltage magnitude and adjusts the set point of DSTATCOM's reactive power reference, whereas the current-base controller compensates for DRs' unbalanced load current by injecting signals through the quadrature axis (q-axis) and zero axis (0-axis) of VSC current controllers. The voltage-base technique controls the voltage drop at the PCC, while the current-base strategy handles the unbalanced current of scattered resources.

Several linear and nonlinear load switching, unbalanced load, and fault situations in a microgrid were simulated to evaluate the proposed technique's capabilities. When the PCC voltage exceeds the intended value during load switching, the voltage-base controller may boost the PCC voltage by modifying the DSTATCOM reactive power generation reference. However, the current-base control approach addressed current imbalances by injecting reference signals into the PWM's q and zero axes. The simulation results for several scenarios demonstrated the efficiency of the proposed online secondary control mechanism.

VII. FUTURE SCOPE

1. Advanced Machine Learning Algorithms: In addition to reinforcement learning, consider deep learning, fuzzy logic, or hybrid techniques. These may improve the control performance and flexibility of DSTATCOMs.
2. Integration with Renewable Energy Sources: As more microgrids include renewable energy sources (RES), future study might look into how DSTATCOMs can efficiently handle RES integration. This includes managing intermittent generation, voltage changes, and harmonics.
3. Real-Time Implementation and Field Trials: The transition from simulation to real-world deployment is critical. Conduct field tests to confirm the suggested control technique's efficacy under various settings, such as diverse load profiles and fault scenarios.
4. Explore strategies to improve the cybersecurity of DSTATCOMs. Robustness against cyber attacks and resilience during grid disruptions are essential components of practical deployment.
5. Investigate decentralized control systems, in which many DSTATCOMs work together to enhance overall grid stability. Decentralized techniques may improve scalability and fault tolerance.
6. Investigate decentralized control systems, in which many DSTATCOMs work together to enhance overall grid stability. Decentralized techniques may improve scalability and fault tolerance.

REFERENCES

[1] P. K. Kesavan, U. Subramaniam, D. J. Almakhles, and S. Selvam, “Modelling and coordinated control of grid connected photovoltaic, wind turbine driven PMSG, and energy storage device for a hybrid DC/AC microgrid,” Prot. Control Mod. Power Syst., vol. 9, no. 1, pp. 154–167, 2024.

[2] J. de la Cruz, Y. Wu, J. E. Candelo-Becerra, J. C. Vásquez, and J. M. Guerrero, “Review of networked microgrid protection: Architectures, challenges, solutions, and future trends,” CSEE J. Power Energy Syst., vol. 10, no. 2, pp. 448–467, 2024.

[3] Z. Wanpeng, Y. Libin, L. Zhengxi, W. Kai, Z. Weiwen, and L. Qianjie, “Optimization method for multi energy microgrid operation considering carbon emissions,” in 2024 IEEE 8th Conference on Energy Internet and Energy System Integration (EI2), 2024, pp. 5093–5098.

[4] E. Buraimoh et al., “Distributed deep deterministic policy gradient agents for real-time energy management of DC microgrid,” in 2024 IEEE Sixth International Conference on DC Microgrids (ICDCM), 2024, pp. 1–5.

[5] M. Ferrari, M. Starke, J. Smith, B. Ollis, A. Sundararajan, and Y. Garcia, “A networked

microgrid framework and testbed for communication, controls, and optimization testing," in 2024 IEEE Energy Conversion Congress and Exposition (ECCE), 2024, pp. 577–584.

[6] M. Yin, L. Li, H. Yan, M. Ren, J. Wang, and M. Ma, "Application scenario analysis of microgrid based on typical structure classification of microgrid," in 2023 IEEE 6th International Electrical and Energy Conference (CIEEC), 2023, pp. 2711–2716.

[7] V. E. Wissa, A. E. Badawy, and A. El-Guindy, "Fault ride-through in grid-connected DC microgrid to improve microgrid and utility grid performance," in 2023 IEEE PES Conference on Innovative Smart Grid Technologies - Middle East (ISGT Middle East), 2023, pp. 1–5.

[8] A. Hossain et al., "Comparative study of different controllers for offshore DC microgrids," in 2023 IEEE Fifth International Conference on DC Microgrids (ICDCM), 2023, vol. Single, pp. 1–6.

[9] J. De La Cruz, J. C. Vasquez, J. M. Guerrero, E. G. Luna, and J. E. Candelo-Becerra, "Adaptive Multi-Agent-Zonal Protection Scheme for AC Microgrids," in 2023 25th European Conference on Power Electronics and Applications (EPE'23 ECCE Europe), 2023, pp. 1–9.

[10] A. Chatterjee, S. Khatua, and A. Panda, "Solar PV based hybrid AC/DC microgrid design and transient analysis for a university campus," in 2023 IEEE Silchar Subsection Conference (SILCON), 2023, pp. 1–5.

[11] K.-H. Tan, M.-Y. Li, and X.-Y. Weng, "Droop controlled microgrid with DSTATCOM for reactive power compensation and power quality improvement," IEEE Access, vol. 10, pp. 121602–121614, 2022.

[12] P. K. Y. Kundela, M. Mangaraj, and S. K. Sudabattula, "Operation of inductively coupled DSTATCOM for power quality enhancement," in 2022 International Mobile and Embedded Technology Conference (MECON), 2022, pp. 210–214.

[13] Y. Venu, K. Garikapati Annapurna, N. M, and B. J, "DSTATCOM based closed loop controlled wind power plant with self excited induction generator for controlling terminal voltage against load disturbances," in 2022 IEEE Fourth International Conference on Advances in Electronics, Computers and Communications (ICAECC), 2022, pp. 1–6.

[14] U. M. Ngei and P. M. Moses, "Optimal location of DSTATCOM considering different load models using bat algorithm," in 2022 IEEE PES/IAS PowerAfrica, 2022, pp. 1–5.

[15] U. M. Ngei and P. M. Moses, "Performance analysis of DSTATCOM in distribution network for mitigation of harmonics," in 2022 IEEE PES/IAS PowerAfrica, 2022, pp. 1–5.

[16] R. Kaushik, O. P. Mahela, and P. K. Bhatt, "Improvement of power quality in distribution grid with renewable energy generation using DSTATCOM," in 2021 Innovations in Power and Advanced Computing Technologies (i-PACT), 2021, pp. 1–6.

[17] A. M. M. Alzubaidi and N. M. Mohsin, "A critical evolution of multifunctional DSTATCOM for power quality improvement and grid integration of RES in distribution system," in 2021 International Conference on Recent Trends on Electronics, Information, Communication & Technology (RTEICT), 2021, pp. 680–684.

[18] A. Sharma, A. Ram, P. Singhal, and N. Goel, "Power quality enhancement in distribution system using simple peak detection controller based DSTATCOM," in 2021 4th International Conference on Recent Developments in Control, Automation & Power Engineering (RDCAPE), 2021, pp. 286–291.

[19] G. Gangil, S. K. Goyal, A. Saraswat, A. Soni, and M. Srivastava, "Power quality improvement using dstatcom in distribution network," in 2021 International Conference on Control, Automation, Power and Signal Processing (CAPS), 2021, pp. 1–6.

[20] A. Juneja, S. K. Bansal, and P. Singh Jamwal, "Comparative analysis of PWM and hysteresis current controllers for unbalanced non-linear load using DSTATCOM," in 2021 Emerging Trends in Industry 4.0 (ETI 4.0), 2021, pp. 1–7.

[21] C. Kumar, M. K. Mishra, and S. Mekhilef, "A new voltage control strategy to improve performance of DSTATCOM in electric grid," China Electrotech. Soc. Trans. Electr. Mach. Syst., vol. 4, no. 4, pp. 295–302, 2020.

[22] D. Suresh, T. J. Kumar, and S. P. Singh, "Three-level active neutral point clamped DSTATCOM with Interval Type-2 fuzzy logic

controller," in 2020 International Conference on Computer Communication and Informatics (ICCCI), 2020, pp. 1–5.

[23] P. A. Afsher and M. V. Manoj Kumar, "DC-link voltage balancing and regulation of split-capacitor VSI based DSTATCOM," in 2020 IEEE International Conference on Power Systems Technology (POWERCON), 2020, pp. 1–6.

[24] A. N. Hussain, A. J. Ali, and F. S. Ahmed, "Comparison and evaluation between two hybrid systems using renewable sources and DSTATCOM," in 2020 6th International Engineering Conference "Sustainable Technology and Development" (IEC), 2020, pp. 73–79.

[25] M. Mangaraj and J. Sabat, "Two and three-level supported DSTATCOM topologies for compensation analysis," in 2020 International Conference on Computational Intelligence for Smart Power System and Sustainable Energy (CISPSSE), 2020, pp. 1–6.

[26] P. Kumar and D. N. Prabhu, "Performance analysis of fuel cell DSTATCOM," in 2019 Fifth International Conference on Electrical Energy Systems (ICEES), 2019, pp. 1–5.

[27] D. Azhagesan, P. Muthuvel, and S. K. Jeyaraj, "Proficiency estimation of four-leg DSTATCOM for compensating load of arc furnace in the distribution system," in 2019 IEEE International Conference on Clean Energy and Energy Efficient Electronics Circuit for Sustainable Development (INCCES), 2019, pp. 1–5.

[28] S. Ahmad and M. S. Potdar, "Real and reactive power compensation of a power system by using DSTATCOM," in 2019 2nd International Conference on Signal Processing and Communication (ICSPC), 2019, pp. 148–152.

[29] E. Das, A. Bhattacharjee, S. Roy, B. Ganguly, A. Banerji, and S. K. Biswas, "A supervised hybrid algorithm based DSTATCOM to cater to dynamic load changes," in 2019 International Conference on Energy Management for Green Environment (UEMGREEN), 2019, pp. 1–6.

[30] A. Kumar and P. Kumar, "Sliding mode control of DSTATCOM for power quality improvement," in 2019 8th International Conference on Power Systems (ICPS), 2019, pp. 1–6.